Acta Crystallographica Section F
Structural Biology and Crystallization Communications
ISSN 1744-3091

Purification, crystallization and preliminary crystallographic analysis of 3-hydroxyacyl-CoA dehydrogenase from *Caenorhabditis elegans*

Yingzhi Xu[a,b] and Fei Sun[a]*

[a]National Laboratory of Biomacromolecules, Institute of Biophysics, Beijing 100101, People's Republic of China, and [b]University of Chinese Academy of Sciences, Beijing 100049, People's Republic of China

Correspondence e-mail: feisun@ibp.ac.cn

Received 18 January 2013
Accepted 13 March 2013

3-Hydroxyacyl-CoA dehydrogenase (HAD; EC 1.1.1.35) is the enzyme that catalyzes the third step in fatty-acid β-oxidation, oxidizing the hydroxyl group of 3-hydroxyacyl-CoA to a keto group. The 3-hydroxyacyl-CoA dehydrogenase from *Caenorhabditis elegans* (*c*HAD) was cloned, overexpressed in *Escherichia coli* and purified to homogeneity for crystallography. Initial crystals were obtained by the hanging-drop vapour-diffusion method. Optimization of the precipitant concentration and the pH yielded two types of well diffracting crystals with parallelepiped and cuboid shapes, respectively. Complete diffraction data sets were collected and processed from both crystal types. Preliminary crystallographic analysis indicated that the parallelepiped-shaped crystal belonged to space group $P1$, while the cuboid-shaped crystal belonged to space group $P2_12_12_1$. Analyses of computed Matthews coefficient and self-rotation functions suggested that there are two *c*HAD molecules in one asymmetric unit in both crystals, forming identical dimers but packing in distinct manners.

1. Introduction

The metabolism of fatty acids by β-oxidation (FAO) is an important energy source for several tissues including heart, muscle and liver, especially during prolonged fasting. Each cycle of β-oxidation shortens the saturated acyl-CoA by two C atoms and generates one acetyl-CoA, one NADH and one $FADH_2$. The enzyme 3-hydroxyacyl-CoA dehydrogenase (HAD) catalyzes the third reaction of the FAO cycle, which oxidizes the hydroxyl group of L-3-hydroxyacyl-CoA to a keto group (Noyes *et al.*, 1974),

$$\text{L-3-hydroxyacyl-CoA} + \text{NAD}^+ \longleftrightarrow \text{3-ketoxyacyl-CoA} + \text{NADH} + \text{H}^+.$$

Based on the chain length of the substrates, the HAD family is divided into three subclasses: 3-hydroxyacyl-CoA dehydrogenases (HADs), long-chain 3-hydroxyacyl-CoA dehydrogenases (LCHADs) and short-chain 3-hydroxyacyl-CoA dehydrogenases (SCHADs). HADs are soluble dimeric enzymes that exhibit substrate specificity for an acyl-chain length of C_4–C_{10} and were previously referred to as short-chain HADs (He *et al.*, 1989). LCHADs form part of a membrane-associated multifunctional protein that has a preference for substrates with an acyl-chain length of C_{10}–C_{16} (El-Fakhri & Middleton, 1982). SCHADs mainly catalyze the conversion of substrates with a chain length shorter than C_4 (Luo *et al.*, 1995). In contrast to HADs and LCHADs, SCHADs are generally classified into the short-chain dehydrogenase/reductase (SDR) family (He *et al.*, 1998).

Deficiencies in HAD activity have been shown to lead to various metabolic disorders, most often manifested as hypertrophic cardiomyopathy, hypoketotic hypoglycaemia, skeletal myopathy and liver dysfunction (Bennett *et al.*, 1996; Pons *et al.*, 1996; Isaacs *et al.*, 1996). As a soluble mitochondrial matrix protein, HAD was the first identified member of the HAD family and was isolated from sheep liver in the 1950s. In the 1970s, the homogeneous HAD was purified from pig heart muscle in sufficient amounts for crystallographic study (Noyes & Bradshaw, 1973). The human HAD gene was mapped to chromosome 4q22–26 and was sequenced in 1996 (Vredendaal *et al.*,

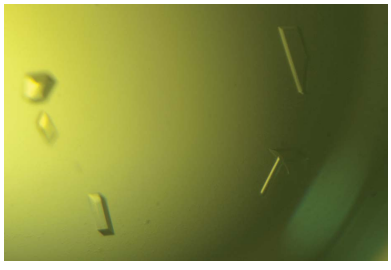

Table 1
Data-collection and processing statistics.

Values in parentheses are for the highest resolution shell.

Crystal	Parallelepiped-shaped	Cuboid-shaped
Space group	*P*1 (No. 1)	$P2_12_12_1$ (No. 19)
Unit-cell parameters (Å, °)	a = 55.7, b = 55.2, c = 56.1, α = 80.5, β = 75.6, γ = 72.4	a = 62.6, b = 96.4, c = 114.2, $\alpha = \beta = \gamma$ = 90
Wavelength (Å)	1.000	1.000
No. of frames collected	720	600
Oscillation angle per frame (°)	0.5	0.3
Exposure time per frame (s)	1.0	1.0
Resolution (Å)	50.00–1.60 (1.63–1.60)	50.00–2.20 (2.24–2.20)
Total reflections	295595	257631
Unique reflections	77082	35658
Multiplicity	3.8 (3.5)	7.2 (7.1)
Completeness (%)	95.6 (92.8)	99.9 (100.0)
$\langle I/\sigma(I)\rangle$	25.42 (3.31)	20.96 (3.28)
$R_{\rm merge}$†	0.033 (0.367)	0.091 (0.366)

† $R_{\rm merge} = \sum_{hkl}\sum_i |I_i(hkl) - \langle I(hkl)\rangle| / \sum_{hkl}\sum_i I_i(hkl)$, where $I_i(hkl)$ is the intensity of the ith observation and $\langle I(hkl)\rangle$ is the mean intensity of reflection hkl.

1996). The crystal structures of both human HAD (Barycki, O'Brien, Bratt *et al.*, 1999) and pig heart HAD (Barycki, O'Brien, Birktoft *et al.*, 1999) contain an N-terminal Rossmann-fold domain (catalytic domain) that comprises the HAD active site with a conserved His–Glu pair and a C-terminal α-helical domain (dimerization domain) that contributes to HAD dimerization. The catalytic mechanism of HAD has been proposed based on the structures of apo, cofactor-bound and substrate-bound human HAD as well as their abortive ternary complex (Barycki *et al.*, 2000). However, the role of subunit dimerization in the HAD catalytic process is largely unknown.

In *Caenorhabditis elegans*, the majority of fat is stored in gut epithelial cells. Lipid droplets have recently been shown to be the fat-storage organelles in *C. elegans* (Zhang *et al.*, 2010). Furthermore, protein F54C8.1 (GenBank accession No. CAA80153.1) from *C. elegans* was predicted to be a 3-hydroxyacyl-CoA dehydrogenase (*c*HAD) and was identified as a novel obesity gene in a randomized RNAi screen in *C. elegans* (Schulz *et al.*, 2011; Ashrafi *et al.*, 2003). Primary amino-acid sequence alignment of 3-hydroxyacyl-CoA dehydrogenases from *C. elegans* and human shows that both catalytic and dimerization domains are present in *c*HAD and that the full-length *c*HAD sequence shares 49% identity with human HAD. In our study, *c*HAD was cloned from a *C. elegans* cDNA library and over-expressed in *Escherichia coli* for biochemical and structural studies. The aim of our study is to use *c*HAD as a model protein to understand how the subunit dimerization of HAD affects its catalytic activity. Two types of well diffracting *c*HAD crystals belonging to different space groups were obtained and their crystal structures were solved by molecular replacement. Further structure analysis and functional study have been performed (to be published elsewhere). Here, we report the cloning, expression, crystallization and preliminary crystallographic analysis of *c*HAD.

2. Materials and methods

2.1. Molecular cloning, protein expression and purification

The gene encoding HAD from *C. elegans* (GenBank accession No. CAA80153.1) was amplified using the PCR technique from a *C. elegans* cDNA library using the forward primer 5′-TTG-GATCCATGTTCACAGCAAAGTGTGCCAT-3′ and the reverse primer 5′-CCGAATTCTTTCTTGTACGAGTAGAATCCGT-3′. After *Bam*HI and *Eco*RI double digestion, the amplified PCR product was ligated into pEXS-CG vector, a vector developed in our laboratory and based on pET-22b(+) vector (Novagen). This recombinant plasmid encodes a fusion protein with a C-terminal GST tag linked by a PreScission Protease (PPase) recognition site. Once the integrity of the PCR product had been verified by sequencing, the plasmid was used to transform *E. coli* strain BL21 (DE3) for protein expression.

The bacteria were cultured in 2×YT medium with 100 µg ml^{-1} ampicillin until the OD_{600} reached approximately 1.0; recombinant protein expression was then induced by the addition of 0.5 m*M* IPTG for 16 h at 289 K. The cell pellets were lysed by sonication in PBS buffer and centrifuged at 15 000*g* for 30 min to yield the soluble fraction. The supernatant was loaded onto a pre-equilibrated GST affinity column (Glutathione Sepharose 4 FF, GE Healthcare) and the column was then washed with PBS buffer containing 1 *M* sodium chloride. After equilibration with buffer *P* [50 m*M* Tris pH 7.0, 150 m*M* sodium chloride, 1 m*M* EDTA, 10%(*v*/*v*) glycerol], the resin was incubated with 100 µg PPase overnight at 277 K for removal of the GST tag. The processed *c*HAD protein eluted from the resin using buffer *P* was collected for further purification.

The protein sample was injected onto a HiTrap Desalting column [1.6 cm (diameter) × 2.5 cm; GE Healthcare] and eluted using buffer *A* (25 m*M* sodium acetate trihydrate pH 5.0, 1 m*M* EDTA) at a flow rate of 1 ml min^{-1} to remove sodium chloride. The desalted protein sample was then subjected to a Resource S ion-exchange column [6.4 mm (inner diameter) × 30 mm; GE Healthcare] in buffer *A* and eluted with a linear sodium chloride gradient at a flow rate of 1 ml min^{-1}. The *c*HAD fractions eluted at approximately 300 m*M* sodium chloride and were pooled and concentrated to 16 mg ml^{-1} by ultrafiltration with molecular-weight cutoff 10 kDa (Millipore).

2.2. Gel-filtration chromatography

Gel-filtration chromatography was performed on a BioLogic DuoFlow chromatography system (Bio-Rad) using a Superdex 200 column (10/300 GL; GE Healthcare). The column was equilibrated with a mobile phase consisting of 25 m*M* Tris pH 7.0, 150 m*M* sodium chloride, 10%(*v*/*v*) glycerol. 600 µg protein was injected onto the column and eluted at a flow rate of 0.5 ml min^{-1}. The column effluent was monitored by ultraviolet (UV) absorption at a wavelength of 280 nm.

2.3. Crystallization and optimization

Crystallization of *c*HAD was performed at 291 K using the hanging-drop vapour-diffusion method. A 1 µl aliquot of protein solution (10 mg ml^{-1}) buffered in 25 m*M* sodium acetate trihydrate pH 5.0 and 300 m*M* sodium chloride was mixed with an equal volume of reservoir solution and equilibrated against 200 µl reservoir solution. Initial screening was performed using the Index screen (Hampton Research). Crystals appeared within 3 d from 13 conditions of the Index screen (Nos. 39, 42, 43, 44, 46, 47, 71, 72, 78, 79, 80, 90 and 96). Based on condition No. 72, optimization was carried out by varying the precipitant concentration and buffer pH value, yielding large single crystals that diffracted to higher than 2.5 Å resolution using an FR-E SuperBright copper rotating-anode X-ray generator (Rigaku, Japan) equipped with a 300 mm R-AXIS IV^{++} image-plate detector (Rigaku, Japan).

2.4. Data collection and processing

The crystals were soaked in a cryoprotectant consisting of 15% PEG 3350, 0.3 *M* sodium chloride and 20% glycerol and were flash-

cooled at 100 K in a stream of nitrogen gas. The high-resolution diffraction data set was collected on beamline BL5A at the Photon Factory (KEK, Japan) using radiation of wavelength 1.0 Å without any attenuation of the beam. A Quantum 315 CCD detector with an active area of 315 × 315 mm was used and all diffraction images were processed using the *HKL*-2000 package (Otwinowski & Minor, 1997). Data-collection and processing statistics are summarized in Table 1.

2.5. Self-rotation function calculation

A self-rotation function was calculated by *MOLREP* (Vagin & Teplyakov, 2010) in the resolution range 50.0–5.0 Å; the integration radius was set to 30 Å.

3. Results and discussion

The *c*HAD recombinant protein was intensively purified to approximately 99% purity using GST affinity and ion-exchange chromatography as judged by SDS–PAGE (Fig. 1*a*). Gel filtration showed that the peak elution volume of *c*HAD was smaller than the GST dimer (52 kDa; Fig. 1*b*). Considering that the molecular weight of *c*HAD monomer is 34.7 kDa, the gel-filtration experiment suggested that *c*HAD exists as a dimer or an oligomer in solution.

Initial screening (25% PEG 3350, 0.2 *M* sodium chloride, 0.1 *M* HEPES pH 7.5) yielded *c*HAD crystals with high mosaicity which were not suitable for data collection (Fig. 2*a*). By using a lower precipitant concentration and optimized pH value, two types of well diffracting crystals were obtained. Using 21% PEG 3350, 0.2 *M* sodium chloride, 0.1 *M* MES pH 6.5, parallelepiped-shaped crystals appeared after 3 d (Fig. 2*b*), while using 23% PEG 3350, 0.2 *M* sodium chloride, 0.1 *M* Bicine pH 8.0, cuboid-shaped crystals appeared after 5 d (Fig. 2*c*, indicated by arrows).

X-ray diffraction data sets were collected from the parallelepiped-shaped and cuboid-shaped crystals on beamline BL5A of the Photon Factory and processed to 1.6 and 2.2 Å resolution, respectively (Figs. 3*a* and 3*b*). The parallelepiped-shaped crystals belonged to space group *P*1, with unit-cell parameters a = 55.7, b = 55.2, c = 56.1 Å, α = 80.5, β = 75.6, γ = 72.4°, while the space group of the cuboid-shaped crystals was $P2_12_12_1$, with unit-cell parameters a = 62.6, b = 96.4, c = 114.2 Å, $\alpha = \beta = \gamma = 90°$ (Table 1). By analyzing the

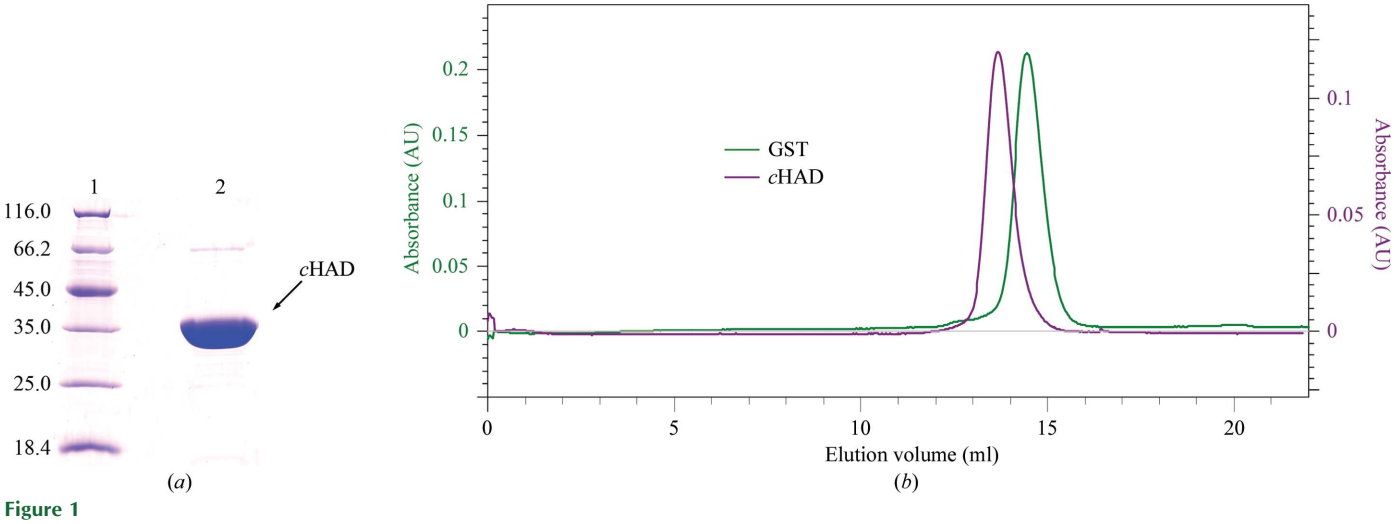

Figure 1
Characterization of purified *c*HAD. (*a*) SDS–PAGE of purified *c*HAD. Lane 1, protein molecular-weight marker (Fermentas); lane 2, purified *c*HAD. SDS–PAGE was performed on a 12%(*w*/*v*) gel and stained using Coomassie Brilliant Blue. (*b*) Gel-filtration chromatography profiles of GST (green) and *c*HAD (purple).

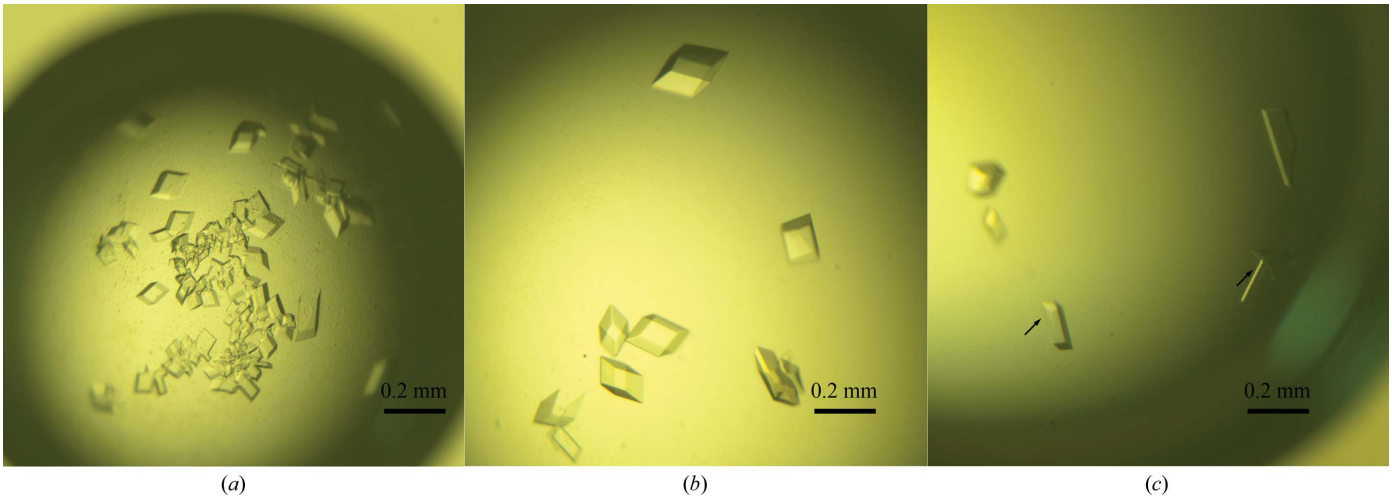

Figure 2
Crystallization of *c*HAD. (*a*) Crystals of *c*HAD observed using condition No. 72 of the Index screen (Hampton Research). The concentration of the protein solution was 10 mg ml^{-1}. (*b*) Parallelepiped-shaped crystals grown using 21% PEG 3350, 0.2 *M* sodium chloride, 0.1 *M* MES pH 6.5 with a protein concentration of 10 mg ml^{-1}. (*c*) Cuboid-shaped crystals (indicated by black arrows) grown using 23% PEG 3350, 0.2 *M* sodium chloride, 0.1 *M* Bicine pH 8.0 with a protein concentration of 7 mg ml^{-1}.

crystal solvent content using the Matthews coefficient (Matthews, 1968), it was suggested that both of the crystals contained two *c*HAD molecules in the asymmetric unit (Table 2). The rational Matthews coefficient and solvent content of the crystal with space group *P*1 are 2.27 Å^3 Da^{-1} and 45.9%, respectively. The rational Matthews coefficient and solvent content of the crystal with the space group $P2_12_12_1$ are 2.51 Å^3 Da^{-1} and 51.0%, respectively. Furthermore, calculation of the self-rotation function revealed the existence of a noncrystallographic twofold axis in the crystal with space group *P*1. (Fig. 3*c*, indicated by an arrow). However, in the crystal with space group $P2_12_12_1$ only crystallographic twofold screw axes are observed (Fig. 3*d*).

Molecular replacement was used to determine the *c*HAD crystal structure in space group *P*1 using *Phaser* (Read, 2001) with the crystal structure of human HAD (PDB entry 3had; Barycki, O'Brien, Bratt *et al.*, 1999) as an initial model. The top solution (LLG = 163.5, translation-function *Z*-score = 12.8) was used for phase refinement and model building. The same procedures were performed to solve the crystal structure of *c*HAD in space group $P2_12_12_1$, in which we analyzed the crystal packing of *c*HAD molecules and found the

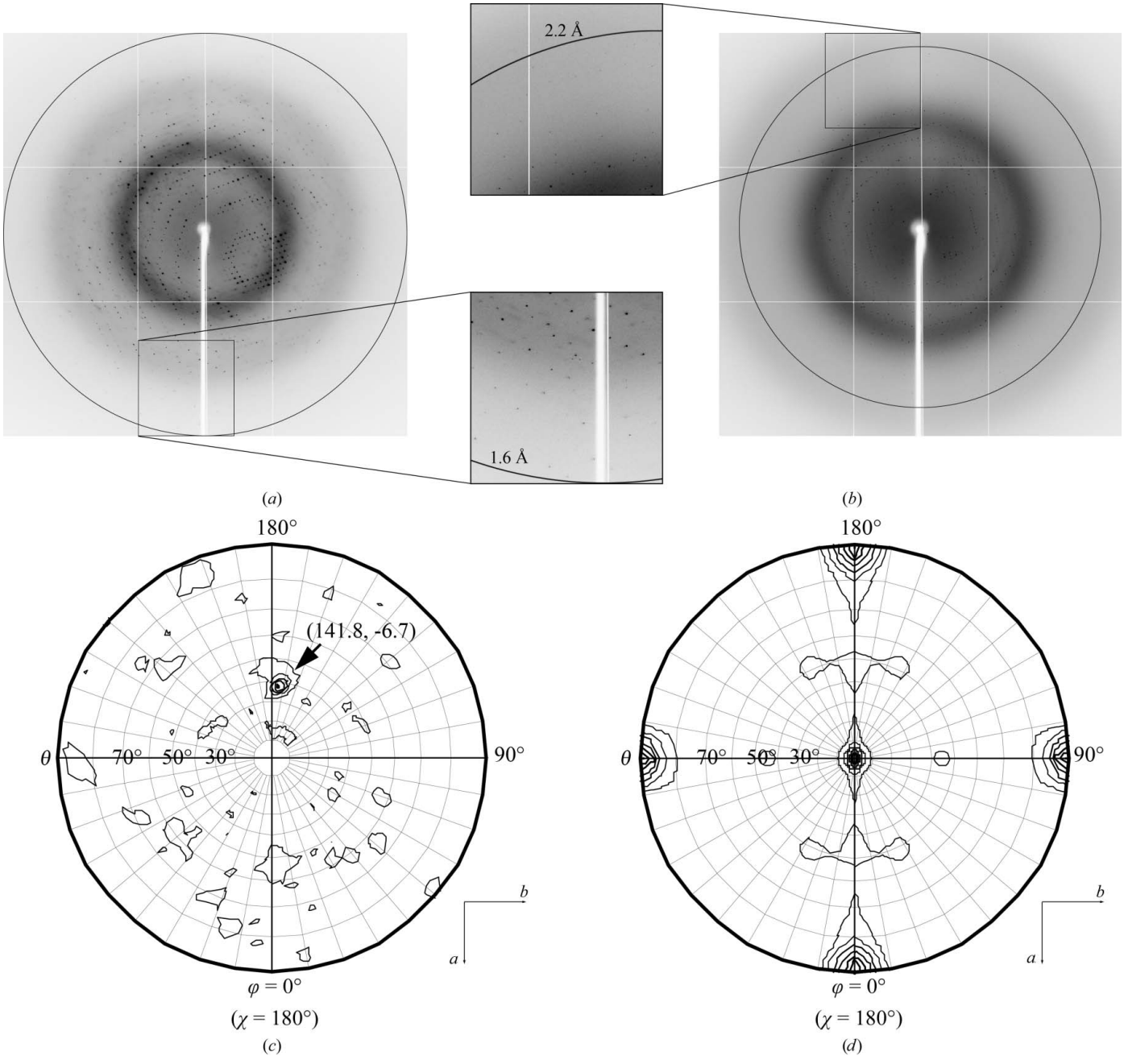

Figure 3
Diffraction of *c*HAD crystals and self-rotation function. (*a*) Diffraction pattern of the parallelepiped-shaped crystal of *c*HAD in space group *P*1. (*b*) Diffraction pattern of the cuboid-shaped crystal of *c*HAD in space group $P2_12_12_1$. The black rings indicate the diffraction limits. (*c*, *d*) Self-rotation function of *c*HAD crystals plotted at $\chi = 180^\circ$ for (*c*) space group *P*1 and (*d*) space group $P2_12_12_1$. Latitude (θ angle) and longitude (φ angle) grid lines are drawn at 10° intervals. The noncrystallographic twofold axis is indicated with a black arrow and its position in (θ, φ) is given in parentheses. The plot is contoured at 22.0σ in (*c*) and 14.0σ in (*d*).

Table 2
Matthews coefficient analysis.

	No. of molecules in asymmetric unit	Matthews coefficient ($Å^3$ Da^{-1})	Solvent content (%)	Probability
*P*1	1	4.55	72.96	0.02
	2	2.27	45.93	0.98
	3	1.52	18.89	0.00
$P2_12_12_1$	1	5.02	75.50	0.01
	2	2.51	50.99	0.98
	3	1.67	26.49	0.01

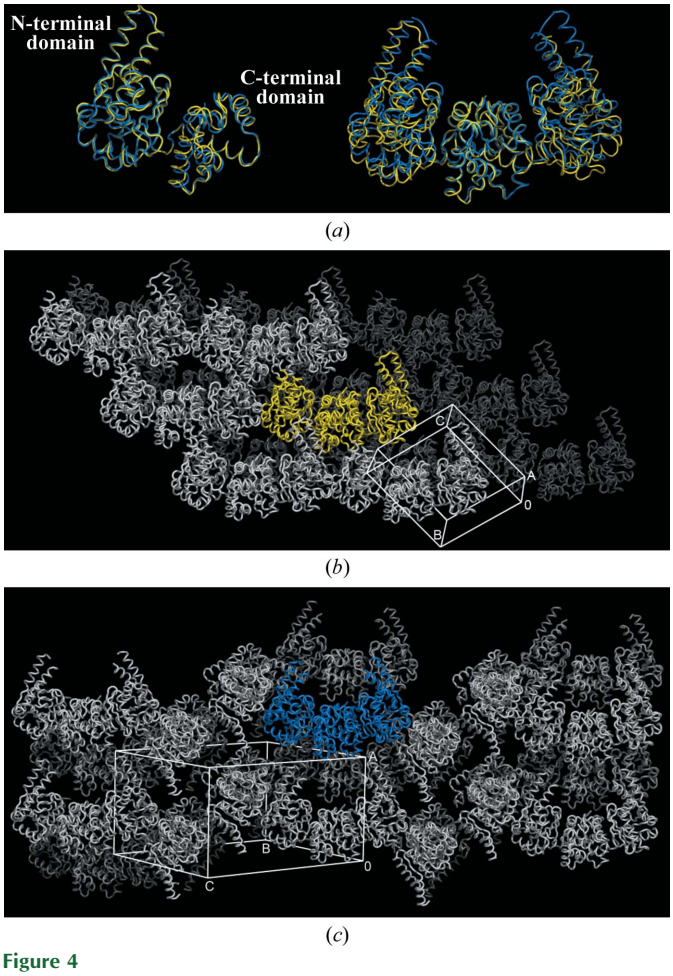

Figure 4
Crystal packing of *c*HAD in different space groups. (*a*) Superpositions of *c*HAD monomers (left) and dimers (right) in space groups *P*1 (yellow) and $P2_12_12_1$ (blue). (*b*) Crystal packing of *c*HAD in space group *P*1. (*c*) Crystal packing of *c*HAD in space group $P2_12_12_1$. These illustrations were generated with *PyMOL* (http://www.pymol.org).

existence of a noncrystallographic twofold axis parallel to the *b* axis. This noncrystallographic twofold symmetry could not be observed from the self-rotation function in space group $P2_12_12_1$ (Fig. 3*d*).

In both space groups *P*1 and $P2_12_12_1$, two monomers contact each other *via* an interaction between C-terminal α-helical domains to form similar dimers (Fig. 4*a*). However, the crystal packing of *c*HAD differs between the crystals in space groups *P*1 and $P2_12_12_1$. In space group *P*1 the *c*HAD dimers pack against each other in a parallel way to form layers (Fig. 4*b*). In space group $P2_12_12_1$ the crystal packing of *c*HAD resembles a pattern similar to the Greek letter π in the way that one dimer is positioned perpendicular to a pair of parallel dimers (Fig. 4*c*). The *c*HAD dimer can thus use different contact surfaces to form two kinds of packing and crystallize in space groups *P*1 and $P2_12_12_1$.

Detailed structural analysis and biochemical studies of *c*HAD will be published elsewhere. The high-resolution structure of *c*HAD and the conformational differences between the two crystal forms will provide new insights into the catalytic mechanism and regulation of the HAD family.

We sincerely thank Professor Weimin Gong for the gift of the *C. elegans* cDNA library and Dr Zhijie Li for the cloning of the *c*HAD cDNA. We also thank Dr Yujia Zhai for help in diffraction data collection and Kai Zhang (from the group of FS) for help with self-rotation function calculation. This work was supported by the '973' program of the Chinese Ministry of Science and Technology (No. 2011CB910301) and the National Natural Science Foundation of China (No. 31021062).

References

Ashrafi, K., Chang, F. Y., Watts, J. L., Fraser, A. G., Kamath, R. S., Ahringer, J. & Ruvkun, G. (2003). *Nature (London)*, **421**, 268–272.
Barycki, J. J., O'Brien, L. K., Birktoft, J. J., Strauss, A. W. & Banaszak, L. J. (1999). *Protein Sci.* **8**, 2010–2018.
Barycki, J. J., O'Brien, L. K., Bratt, J. M., Zhang, R., Sanishvili, R., Strauss, A. W. & Banaszak, L. J. (1999). *Biochemistry*, **38**, 5786–5798.
Barycki, J. J., O'Brien, L. K., Strauss, A. W. & Banaszak, L. J. (2000). *J. Biol. Chem.* **275**, 27186–27196.
Bennett, M. J., Weinberger, M. J., Kobori, J. A., Rinaldo, P. & Burlina, A. B. (1996). *Pediatr. Res.* **39**, 185–188.
El-Fakhri, M. & Middleton, B. (1982). *Biochim. Biophys. Acta*, **713**, 270–279.
He, X.-Y., Schulz, H. & Yang, S.-Y. (1998). *J. Biol. Chem.* **273**, 10741–10746.
He, X.-Y., Yang, S.-Y. & Schulz, H. (1989). *Anal. Biochem.* **180**, 105–109.
Isaacs, J. D., Sims, H. F., Powell, C. K., Bennett, M. J., Hale, D. E., Treem, W. R. & Strauss, A. W. (1996). *Pediatr. Res.* **40**, 393–398.
Luo, M. J., Mao, L. F. & Schulz, H. (1995). *Arch. Biochem. Biophys.* **321**, 214–220.
Matthews, B. W. (1968). *J. Mol. Biol.* **33**, 491–497.
Noyes, B. E. & Bradshaw, R. A. (1973). *J. Biol. Chem.* **248**, 3052–3059.
Noyes, B. E., Glatthaar, B. E., Garavelli, J. S. & Bradshaw, R. A. (1974). *Proc. Natl Acad. Sci. USA*, **71**, 1334–1338.
Otwinowski, Z. & Minor, W. (1997). *Methods Enzymol.* **276**, 307–326.
Pons, R., Roig, M., Riudor, E., Ribes, A., Briones, P., Ortigosa, L., Baldellou, A., Gil-Gibernau, J., Olesti, M., Navarro, C. & Wanders, R. J. (1996). *Pediatr. Neurol.* **14**, 236–243.
Read, R. J. (2001). *Acta Cryst.* D**57**, 1373–1382.
Schulz, N., Himmelbauer, H., Rath, M., van Weeghel, M., Houten, S., Kulik, W., Suhre, K., Scherneck, S., Vogel, H., Kluge, R., Wiedmer, P., Joost, H. G. & Schürmann, A. (2011). *Endocrinology*, **152**, 4641–4651.
Vagin, A. & Teplyakov, A. (2010). *Acta Cryst.* D**66**, 22–25.
Vredendaal, P. J., van den Berg, I. E., Malingré, H. E., Stroobants, A. K., Olde Weghuis, D. E. & Berger, R. (1996). *Biochem. Biophys. Res. Commun.* **223**, 718–723.
Zhang, S. O., Trimble, R., Guo, F. & Mak, H. Y. (2010). *BMC Cell Biol.* **11**, 96.